INDIAN JOURNAL OF SCIENCE AND TECHNOLOGY

RESEARCH ARTICLE

Aniline Formaldehyde Cross-Linked Polyaniline Magnetic Nanocomposite with Core-Shell Structure As A New Platform for Enzyme Immobilization

Maria Augustine[1,2], G Geetha[1], T M Dhanya[1], G Anjali Krishna[1], P V Mohanan[3]*

1 Research Scholar, Department of Applied Chemistry, CUSAT, Kalamassery, India
2 Department of Chemistry, St.Paul's College, Kalamassery, India
3 Professor, Department of Applied Chemistry, CUSAT, Kalamassery, India

OPEN ACCESS

Received: 04-10-2022
Accepted: 10-05-2023
Published: 31-05-2023

Citation: Augustine M, Geetha G, Dhanya TM, Krishna GA, Mohanan PV (2023) Aniline Formaldehyde Cross-Linked Polyaniline Magnetic Nanocomposite with Core-Shell Structure As A New Platform for Enzyme Immobilization. Indian Journal of Science and Technology 16(21): 1555-1562. https://doi.org/10.17485/IJST/v16i21.1977

* **Corresponding author**.

mohan@cusat.ac.in

Funding: Maria Augustine is thankful to CSIR-JRF for the financial support at the initial stage of studies

Competing Interests: None

Published By Indian Society for Education and Environment (iSee)

ISSN
Print: 0974-6846
Electronic: 0974-5645

Abstract

Objectives: The industrial application of an enzyme is governed by its thermodynamic properties and stability, which can be effectively improved by immobilizing enzymes onto suitable supports. The present work is done by immobilizing α-amylase onto aniline formaldehyde condensate cross-linked polyaniline magnetic nanocomposite. **Methods:** Physiochemical characterization of synthesized Fe_3O_4-CLPANI nanocomposite was done by FT-IR, XRD, TG, and SEM images. Biochemical characterization related to immobilization efficiency, the kinetic parameters Vmax and the Km value, thermal stability, storage stability and reusability of immobilized enzymes were determined. **Findings:** Both physiochemical and biochemical characterization led to the conclusion that Fe_3O_4–CLPANI immobilized amylase indicated better thermal stability than that of free enzyme and it tailored to the requirement as an industrial catalyst. **Novelty:** To the best of our knowledge, no literature is available on the immobilization of the enzyme to Fe_3O_4–CLPANI composites with core-shell structure.

Keywords: Nanocomposite; Amylase; Immobilization; Thermal stability; Thermal deactivation α

1 Introduction

Biomolecules, especially enzymes, have received great attention nowadays as they are widely used for catalyzing many chemical reactions in complex environments. However, their commercial use is often restricted due to poor operating stability, high consumption, low controllability and non-reusability. Enzyme immobilization has been proven to be the most successful strategy for addressing these issues, improving catalytic stability, separation, and reutilization for numerous cycles, making them commercially and industrially feasible[(1,2)]. A wide range of carriers has been used for the immobilization of enzymes[(3)]. Polymer magnetic nanocomposites have earned an unavoidable place in all branches of research and are used for a variety

of applications, including medication administration, sensors, and contrast agents in magnetic resonance imaging due to their exceptional and peculiar magnetic properties, improved performance and large surface area[4–6].

Nowadays many studies have focused on the preparation of a wide variety of composites with magnetic and conducting properties. Recently Congqiang Lou et al. utilized Magnetic graphene nanocomposites to immobilize laccase[7]. M.Cabrera et al. presented a simple, cost-effective, and efficient method for making a composite out of magnetic diatomaceous earth (mDE) coated with polyaniline (mDE@PANI) which was utilized to immobilize invertase, galactosidase, and trypsin[8]. Several studies have been published in which different polyaniline magnetite composites were utilized as effective support for enzyme immobilization, dye absorption studies, and heavy metal absorption.[4] Fe_3O_4 particles can be wrapped in PANI to create new nanomaterials with a core-shell structure and fascinating magnetic and electrical characteristics. One disadvantage observed was that the use of these composites in acidic solutions is limited because the magnetic core-shell dissolves in acidic solutions and loses its magnetic property. Wan's group produced a core-shell Fe_3O_4 cross-linked polyaniline (CLPANI) nanocomposite by using aniline formaldehyde condensate during aniline polymerization, wherein cross-linked PANI serves as the conductive shell and Fe_3O_4 serves as the magnetic core[9,10]. To the best of our knowledge, no literature is available on the immobilization of enzymes to Fe_3O_4–CLPANI composites with core-shell structure.

One of the numerous amylase enzymes, α-amylase (1,4-d-glucanglucanhydrolase, EC.3.2.1.1), hydrolyzes starch to maltose by randomly cleaving the internal 1,4-linkages (endoamylase). α-amylase is an enzyme used in several industrial sectors, including the production of ethanol. high fructose corn syrup, and paper recycling[11,12]. Adsorption based on physical adsorption or ion binding is the most basic and popular method used in the immobilization process. The benefit of this approach is that it lessens interference from the inactive centre, preserving the full level of activity[13].

In the current study, precipitation oxidation was primarily used to create the Fe_3O_4 nanoparticles. Fe_3O_4-CLPANI nanocomposites with the core-shell structure were then created by *in-situ* polymerizing aniline monomer and AFC in an aqueous solution that contained a dispersion of Fe_3O_4 nanoparticles. By using Fe_3O_4-CLPANI composites with a core-shell structure as a carrier, -amylase was immobilized. XRD, IR, TGA and SEM analyses were used to characterize the produced Fe_3O_4–CLPANI composites. For the best immobilization yield and efficiency, the impacts of several immobilization parameters, including temperature, pH, contact time, and the amount of enzyme needed, were investigated. The kinetic parameters K_m and V_{max} were computed using the Lineweaver Burk graph and Hanes Woolf graph. The reusability, thermal stability, and storage stability of the enzyme were investigated in both free and immobilized conditions.

2 Materials and Methods

2.1 Materials

Aniline ($C_6H_5NH_2$), Formaldehyde (HCHO), Iron (II) sulfate. Heptahydrate ($FeSO_4.7H_2O$), Iron (III) chloride. Hexahydrate ($FeCl_3.6H_2O$), and soluble potato starch were obtained from S.D. Fine Chem. Ltd., Mumbai. Diastase α-amylase (1,4 α-D-gluconglucanohydrolse, E. C. 3.2.1.1) was bought from Hi-Media Laboratories Pvt. LTD., Mumbai. Ammonia solution (NH_3, 25%), acetone, Hydrochloric acid (HCl) and Ammonium peroxodisulphate (APS) were purchased from Merck Co. Aniline monomer was distilled at low pressure and kept at temperatures below 0 °C. The remaining reagents were of analytical quality and were utilized without additional purification.

2.2 Preparation of Fe_3O_4-CLPANI Nanocomposite

Fe_3O_4 nanoparticles were prepared according to the method by Bruce et al.[14] and aniline formaldehyde condensate (AFC) was prepared according to the method of Liu et al.[15]. (supplementary data- Appendix A2). Fe_3O_4–CLPANI nanocomposite was prepared according to the literature[16] with a few modifications via *in-situ* polymerization of aniline monomer and aniline formaldehyde condensate in an aqueous solution containing magnetite (Detailed method of preparation is given in **s**upplementary data – Appendix A3).

2.3 Characterization of Fe3O4-CLPANI Nanocomposite

The nanocomposite was analyzed using the KBr pellet technique on a JASCO FT-IR 4100 spectrometer at room temperature, with absorption bands recorded in the 500-4000cm^{-1} range. XRD analysis of the composite was done by Bruker AXS D8 Advance. Thermal decomposition study of the composite was performed by TG- DTG analysis using Perkin Elmer Pyris Diamond TG analyzer. The surface morphology of the nanocomposite was examined using a JEOL Model JSM-6390LV scanning electron microscope.

2.4 Immobilization of Alpha-Amylase

For maximum activity and immobilization yields, immobilization parameters including temperature, enzyme concentration, immobilization medium pH, and enzyme contact time were optimized. By combining the nanocomposite with equal quantities of enzyme solution and buffer at optimum conditions, the enzyme alpha-amylase was immobilized onto the nanocomposite. It was shaken to eliminate the unattached enzyme; it was washed twice using the same buffer. The supernatant and washings were collected to perform a total protein assay using Lowry's technique[17]. A Thermo scientific evolution 201 UV-Visible Double Beam Spectrophotometer was used to measure the absorbance of Folin-phenol Ciocaltaue's reagent at 660 nm.

2.5 Activity determination of the free and immobilized enzyme

Using starch as a substrate, Fuwa's method was used to determine the activity of the immobilized and free enzymes[18,19] (Supplementary data – Appendix A4).

The loss of an average of 1 mg of iodine-binding starch material per minute in the assay response is known as the starch-iodine assay. Consequently, Equation (1) was used to compute the activity(U/mL).

$$Activity\ \left(\frac{U}{mL}\right) = \frac{A_{650}\ control - A_{650}\ sample}{Absorbance\ for\ 1\ mg\ of\ starch\ derived\ from\ the\ standard\ curve\ \times incubation\ time\ \times Volume\ of\ the\ enzyme\ (mL)}$$

A_{650} sample is the absorbance for the starch digested with the enzyme, as opposed to A_{650} control, which is the absorbance obtained from the starch without the addition of an enzyme .

2.6 Calculation of Immobilization Yield, Activity Yield and Immobilization Efficiency

Equation (2) was used to compute immobilization yield (IY) by comparing the protein concentration of the supernatant before and after immobilization.

$$IY(\%) = \frac{C1 - C2}{C1} \times 100 \tag{2}$$

Where C_1 was the protein concentration used for immobilization and C_2 was the protein concentration in the supernatant following immobilization.

And the activity yield (AY) was determined by Equation (3),

$$AY(\%) = \frac{Activity\ of\ immobilized\ enzyme}{Activity\ of\ free\ enzyme} \times 100 \tag{3}$$

The immobilization efficiency (IE) was calculated using Equation (4),

$$IE(\%) = \frac{AY}{IY} \times 100 \tag{4}$$

2.7. Comparative studies of free and immobilized enzyme

2.7.1. Effect of pH on enzyme activity

The pH of the reaction affects the activity of free and immobilized enzymes and this was studied using acetate buffer (pH 4 - 5.5), phosphate buffer (pH 6-8) and glycine buffer (8.5-9) at room temperature over a pH range of 4-9. This was done by stirring a definite amount of free and immobilized enzyme in a suitable buffer with 1% starch solution as the substrate for 15 minutes at 30 °C. An enzyme assay was performed as in the determination of free and immobilized enzyme activity explained above.

2.7.2. Effect of temperature on enzyme activity

By adjusting the temperature between 30°C and 70°C, the best temperature for the maximum activity of the free and immobilized enzymes was investigated. Plotting the log of the relative activity of the measured temperature versus 1/T (Kelvin) for the free and immobilized samples, the activation energy, E_a is calculated from the slope of the Arrhenius plot in accordance with Equation (5), where R is the gas constant (8.314 kJ/mol) and T is the absolute temperature (Kelvin).

$$\text{Slope} = E_a/2.303R \tag{5}$$

2.7.3. Determination of Thermal stability

The enzyme samples were subjected to different temperatures (30-70º C) at optimum pH for a pre-incubation period of 2 h, and the residual activity was then measured with the starch as the substrate at optimum pH and optimum temperature.

2.7.4 Kinetic studies of free and immobilized alpha-amylase

Under ideal pH and temperature circumstances, initial reaction rates were observed by adjusting the substrate concentration. The Michaelis-Menten constant (K_m) value represents the enzyme's affinity for the substrate, and the maximum rate of the enzymatic reaction (V_{max}), represents the number of molecules of substrate transformed into product per minute per enzyme molecule. Both the parameters can be evaluated from the Lineweaver-Burk plot using the Equations (6) and (7) respectively.

$$V_{max} = 1/\text{y-intercept} \tag{6}$$

$$Km = \text{slope} * V_{max} \tag{7}$$

2.7.5 Reusability and storage stability

The reusability of the immobilized enzyme was tested using a batch experiment with fixed times for each cycle. At the optimal pH and temperature, the immobilized enzyme's residual activity was assessed at regular intervals. At the end of each cycle, the immobilized enzyme was removed, washed with buffer, and a substrate solution was added to start a new cycle. The process is repeated after each count.

During four weeks of storage at 4°C, the activity of immobilized enzymes in buffer solution was assessed at regular intervals. The % activity was obtained by comparing the final activity to the initial one.

3 Result and discussion

3.1. Structural characterization of Fe_3O_4-CLPANI nanocomposite

FT-IR spectra of Fe_3O_4 and Fe_3O_4-CLPANI composite (**Supplementary data- Appendix B- Figure B1**)

The -NH stretching vibration is represented by the absorption peak at 3500-3000 cm^{-1} and the -CH stretching vibration by faint absorption bands at 2800-3150 cm^{-1} [20]. The absorption peak of 3419.6 cm^{-1} in magnetite spectra corresponds to the hydroxyl group on the Fe_3O_4 magnetic nanoparticle surfaces, which led to the surface modification of nanoparticles [21]. The peaks of CLPANI in the composite mask the above peak of magnetite, which confirms the encapsulation of the magnetic nanoparticle by CLPANI and indicates the bonding of CLPANI strongly to the surface hydroxyl groups on the magnetic nanoparticle. The peaks in the region 1588 cm^{-1} and 1489 cm^{-1} are the C=C and C=N stretching deformation of quinoid, (N=Q=N)and C-N stretching vibrations respectively and show a shift to lower wave number on comparing the corresponding peaks of polyaniline. The N atom in the CLPANI chain may interact with the Fe atom's 3d orbit to form a coordinate bond, which might reduce the interval between the phenyl ring's energy levels [21]. The vibration absorption peak of the Quinone nitrogen atom in Fe_3O_4-CLPANI is 1145 cm^{-1}, indicating that CLPANI has been effectively coated onto the surface of Fe_3O_4 particles. The peaks below 1000 cm^{-1} especially the peak in the composite at 570 cm^{-1} are related to the Fe-O bond vibration of Fe_3O_4 which shows the presence of magnetite in the composite [16]. Furthermore, the strength of the characteristic peaks of PANI at 2813.1 and 2926.5 cm^{-1} reduced, indicating some interaction between the active sites on the PANI surface and the Fe_3O_4 particles. Interactions between PANI and Fe_3O_4 particles in composite materials were also found in a minor change in percentage transmittance towards longer wavelength regions, as previously described [22]. The presence of physical forces between CLPANI and Fe_3O_4 is demonstrated by the movement of absorption bands toward low frequency. In the FTIR spectra of Fe_3O_4-CLPANI composites, the band at 3400 cm^{-1} has been replaced by a large absorption plateau [16,23].

All the diffraction peaks of the XRD spectrum of Fe_3O_4-CLPANI composites (Supplementary data- Appendix B- Figure B2), with main peaks at 2θ values 30.20^0, 35.86^0, 43.61^0,54.17^0,57.56^0, 62.74^0 were in good agreement with the face-centered cubic structure (fcc) of magnetite (JCPDS 199-629) [16]. The diminished intensity of peaks compared to that of pure magnetite indicates that the surface of magnetite is successfully modified by CL-PANI coating, and the magnetite structure is well retained in the composite even after coating in acidic conditions. The average particle size of the Fe_3O_4-CLPANI composite was calculated using Debye Sherrer equation and was found to be 7.43 nm [8,21].

(Supplementary data- Appendix B- Figure B3) gives scanning electron microscope images of Fe_3O_4-CLPANI nanocomposite. The polymer is aggregated with near-spherical morphology and distributed non-uniformly resulting in the encapsulation of magnetic nanoparticles by CLPANI. The magnetite was completely covered by the CL-PANI which was revealed by the rough surface morphology of the composite.

The TG and DTG curves of Fe_3O_4-CLPANI (Supplementary data- Appendix B- Figure B4) composite exhibited three major weight losses. The initial phase of weight loss below 200^0 C was related to the elimination of physically-sorbed water and dopant anion from CL-PANI. The second stage is around 200^0 C and 320^0C due to the loss of water and HCl which are bonded to the polymer chain. The third stage of weight loss at 425^0C is due to the decomposition of the polymer chain. This points to the increased thermal stability of Fe_3O_4-CLPANI composite which can be due to the interaction of polymer chain and nano magnetite particle [21].

3.2. Optimization of Immobilisation of free enzymes

Immobilization parameters such as pH, contact period, initial amount of protein and temperature were optimized (Supplementary data – Appendix C1-C4) and evaluated the immobilization yield, activity yield, and immobilization efficiency of the immobilized enzyme (Table 1) [19,24]. The maximum activity was observed at immobilization pH 7, contact period of support and enzyme at 60 minutes, initial amount of protein of 1mg and immobilization temperature of 40°C were taken as the optimum immobilization parameter. [19,25,26].

Table 1. The immobilization yield, activity yield, and immobilization efficiency of immobilized enzyme

Support	Initial protein	Immobilized Protein	Immobilization Yield(%)	Activity Yield (%)	$IE(\%) = \frac{AY}{IY} \times 100$
Fe_3O_4 CL-PANI	1 mg	0.94	94%	90	95.7

3.3 Comparison of performance of free and immobilized α- amylase

3.3.1 Effect of pH on enzyme activity

In the pH range of 4 to 9, the impact of pH and temperature on the activity of -amylase was discovered (**Supplementary data- Appendix D Figure D1**). The free enzyme displayed its highest level of activity at a pH of 5.5 and the immobilized enzyme at a pH of 6. The alkaline shift in the area of optimal pH of immobilized enzyme may be related to the positive charges on the composite's amine group, which may have led to a drop in the H^+ concentration in the microenvironment around the immobilized enzyme. The immobilized enzyme's structural configuration may alter as a result, increasing the enzyme's activity at higher pH levels. The immobilized enzyme exhibited promising pH stability across a wide pH range, which might be attributed to the enzyme's multipoint attachment to the support surfaces [12,19].

3.3.2 Effect of temperature on enzyme activity

The reaction's incubation temperature fluctuated between 30 - 60 ^{0}C. (**Supplementary data- Appendix D- Figure D2**). The relative activity obtained was 86% when the enzyme was immobilized, which shifts its optimal temperature from 50 ^{0}C to 40 ^{0}C, which can be related to a change in the structural integrity of the enzyme structure, which promoted improved amylase activity below 50 ^{0}C. Otherwise, the protein structure may have been altered by the attachment to the support, and higher temperatures may have resulted in the denaturation of the enzyme due to the breakdown of non-covalent intramolecular interactions.The immobilized enzyme exhibited a broad and stable temperature profile and retained more than 50 % activity even at 60 ^{0}C. This can be ascribed to the protective effect provided by the enzyme support at higher temperatures where denaturation occurs [19,24].

The activation energy of immobilized amylase and free amylase for the hydrolysis of the starch substrate can be obtained from the Arrhenius plot for Free enzyme and immobilized enzyme shown in Figure 1. It is found that the free enzyme's activation energy, (E_a = 11.05 kJ mol^{-1}), is lower than that of the immobilized enzyme, (E_a = 36.41 kJ mol^{-1}), due to the prolongation of enzyme and substrate contact and to the changes in the structural conformation of the enzyme by immobilization, which in turn decreases the catalytic efficiency [11].

3.3.3 Determination of Thermal stability

Thermal stability was studied for both free and immobilized forms at varied preincubation temperatures and time intervals. The high thermal stability of the immobilized enzyme is attained by the conformational integrity of the enzyme structure by immobilization with rigid support [11]. (Supplementary data- Appendix D- Figure D3). Even after 2 hours at 80 °C, the immobilized form retained half of its activity, whereas the free enzyme retained just one-fifth of its initial activity.

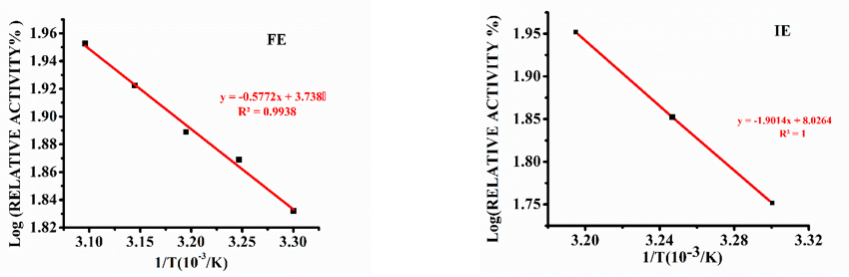

Fig 1. Arrhenius plot for a) free enzyme b) immobilized enzyme

3.3.4 Determination of kinetic parameters

By performing the starch hydrolysis process at optimum temperature and pH for substrate concentrations ranging from 0.2-1.00 mg/mL, the kinetic characteristics of free and immobilized enzymes were examined. The kinetic parameters, K_m, V_{max}offree and immobilized amylase are obtained from the Lineweaver-Burk plot and Hanes Woolf Plot Figure 2 (a) and 2(b) and are shown in shown in Table 2 . Immobilization resulted in a decrease in V_{max} and an increase in K_m, indicating a lower affinity for substrate molecules due to conformational changes in the enzyme caused by excessive adsorption of enzymes on the support, resulting in reduced accessibility of substrate molecules to the enzyme's active site [12].

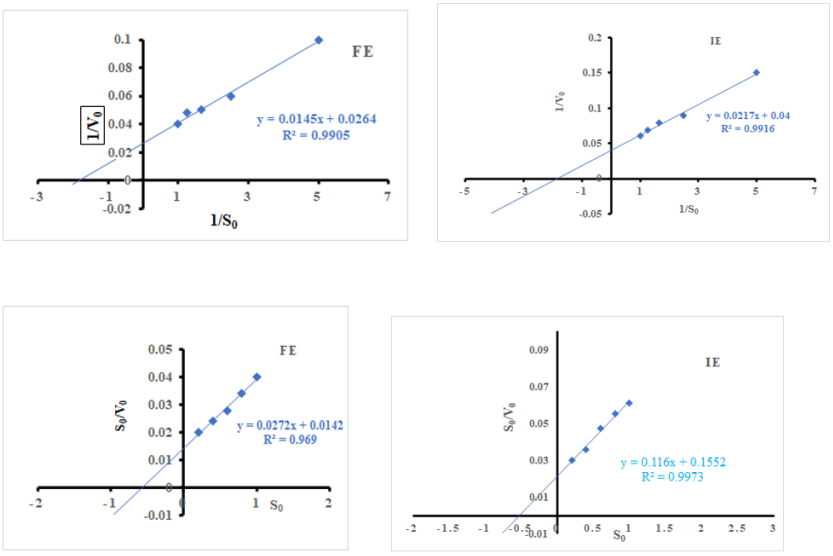

Fig 2. (a). Lineweaver Burk plot for free enzyme and immobilizedenzyme (b). Hanes Woolf plot for free enzyme and immobilized enzyme

Table 2. Comparison of kinetic parameters of free and immobilized enzyme

Kinetic Parameters	Free enzyme	Immobilized enzyme
K_m (mg/mL)	0.54±0.01	0.66±0.02
V_{max} (μmol mg^{-1} min^{-1})	37.87 ±0.03	27.1 ±0.05

3.3.5 Reusability and Storage stability

The reusability of immobilized α-amylase was assayed over twelve reaction cycles at optimum pH and temperature. The relative activity of the first run was set to 100%, and the results are displayed in Figure 3 (a). Immobilized enzyme retained 72% after 6 cycles and 45% after 12 cycles. The results indicated that the catalytic activity of the immobilized enzyme was durable under repeated use. The loss in activity was attributed to the inactivation of the enzyme due to the weakening of the binding strength between the enzyme and the support after continuous use [27].

The storage stability of the immobilized enzyme showed that Immobilized enzyme retained 76% after 2 weeks and 59% after 4 weeks, suggesting that the immobilized enzyme exhibited improved storage stability Figure 3 (b). This is because the immobilization of α- amylase onto Fe_3O_4-CLPANI composite has succeeded to reduce the natural loss of enzyme activity and increased the enzyme's storage stability [12].

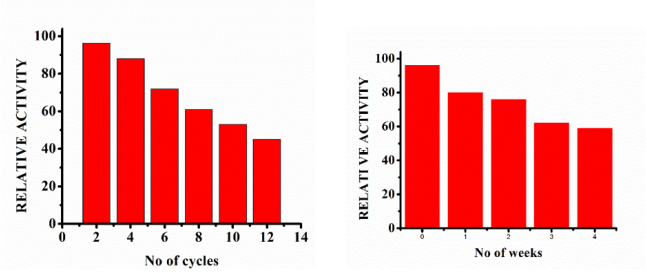

Fig 3. (a) Reusability and (b) Storage stability of the immobilized enzyme

4 Conclusion

Surface encapsulation of magnetite by aniline formaldehyde crosslinked polyaniline was confirmed using FTIR spectra, XRD, TG and SEM. α-amylase was successfully immobilized on Fe_3O_4-CLPANI nanocomposite. The optimum pH and temperature values of α-amylase in magnetite nanocomposite were modified due to the enzyme's conformational change, which could boost the enzyme's applicability. The immobilized enzyme has good storage and reusability properties. These results demonstrate that Fe_3O_4-CLPANI provided good support for α -amylase immobilization. The kinetic characteristics of an enzyme immobilized on Fe_3O_4-CLPANI nanocomposite have been determined. At high temperatures, the activity of the immobilized enzyme was greater than that of the free enzyme. Immobilized enzymes were found to be more robust to environmental conditions than unbound enzymes. Immobilized enzymes were found to be more robust to environmental conditions than unbound enzymes. The study discovered that immobilized enzyme has greater thermal stability than free enzyme and that the Fe_3O_4-CLPANI nanocomposite immobilized enzyme is tailored to the needs of an industrial catalyst.

Acknowledgement

The author Maria Augustine is thankful to CSIR-JRF for the financial support at the initial stage of studies. The authors are thankful to Cochin University of Science and Technology and STIC for providing facilities for this work.

References

1) Basso A, Serban S. Industrial applications of immobilized enzymes—A review. *Molecular Catalysis*. 2019;479:110607. Available from: https://dx.doi.org/10.1016/j.mcat.2019.110607.
2) Mohammadi A, Jafari SM, Mahoonak AS, Ghorbani M. Liposomal/Nanoliposomal Encapsulation of Food-Relevant Enzymes and Their Application in the Food Industry. *Food and Bioprocess Technology*. 2021;14(1):23–38. Available from: https://dx.doi.org/10.1007/s11947-020-02513-x.
3) Yandri Y, Ropingi H, Suhartati T, Hendri J, Irawan B, Hadi S. The Effect of Zeolite/Chitosan Hybrid Matrix for Thermal-stabilization Enhancement on the Immobilization of Aspergillus fumigatus α-Amylase. *Emerging Science Journal*. 2022;6(3):505–518. Available from: https://doi.org/10.28991/ESJ-2022-06-03-06.
4) Darwesh OM, Ali SS, Matter IA, Elsamahy T, Mahmoud YA. Enzymes immobilization onto magnetic nanoparticles to improve industrial and environmental applications. *Methods in Enzymology*. 2020;p. 481–502. Available from: https://dx.doi.org/10.1016/bs.mie.2019.11.006.
5) Gennari A, Führ AJ, Volpato G, De Souza CFV. Magnetic cellulose: Versatile support for enzyme immobilization - A review. *Carbohydrate Polymers*. 2020;246:116646. Available from: https://dx.doi.org/10.1016/j.carbpol.2020.116646.
6) Sheldon RA, Basso A, Brady D. New frontiers in enzyme immobilisation: robust biocatalysts for a circular bio-based economy. *Chemical Society Reviews*. 2021;50(10):5850–5862. Available from: https://doi.org/10.1039/D1CS00015B.
7) Lou C, Jing T, Zhou J, Tian J, Zheng Y, Wang C, et al. Laccase immobilized polyaniline/magnetic graphene composite electrode for detecting hydroquinone. *International Journal of Biological Macromolecules*. 2020;149:1130–1138. Available from: https://doi.org/10.1016/j.ijbiomac.2020.01.248.
8) Cabrera MP, Fonseca TFD, De Souza RVB, De Assis CRD, Marcatoma JQ, Maciel JDC, et al. Polyaniline-coated magnetic diatomite nanoparticles as a matrix for immobilizing enzymes. *Applied Surface Science*. 2018;457:21–29. Available from: https://doi.org/10.1016/j.apsusc.2018.06.238.
9) Wan M, Fan J. Synthesis and ferromagnetic properties of composites of a water-soluble polyaniline copolymer containing iron oxide. *Journal of Polymer Science Part A: Polymer Chemistry*. 1998;36:2749–2755. Available from: https://dx.doi.org/10.1002/(SICI)1099-0518(19981115)36:15%3C2749::AID-POLA11%3E3.0.CO;2-O.

10) Wan M, Li J. Synthesis and electrical-magnetic properties of polyaniline composites. *Journal of Polymer Science Part A: Polymer Chemistry*. 1998;36:2799–2805. Available from: https://dx.doi.org/10.1002/(SICI)1099-0518(19981115)36:15%3C2799::AID-POLA17%3E3.0.CO;2-1.
11) P SD, Unniganapathi B, G G, Mohanan P. Improvement in the Properties of α-Amylase Enzyme by Immobilization using Metal Oxide Nanocomposites as Carriers. 2020. Available from: https://www.researchgate.net/publication/344460042.
12) Bindu VU, Shanty AA, Mohanan PV. Parameters Affecting the Improvement of Properties and Stabilities of Immobilized α-amylase on Chitosan-metal Oxide Composites. *International Journal of Biochemistry and Biophysics*. 2018;6(2):44–57. Available from: https://doi.org/10.13189/ijbb.2018.060203.
13) Hallol M, Helmy O, Shawky AE, El-Batal A, Ramadan M. Optimization of Alpha-Amylase Production by a Local Bacillus paramycoides Isolate and Immobilization on Chitosan-Loaded Barium Ferrite Nanoparticles. *Fermentation*. 2022;8(5):241. Available from: https://doi.org/10.3390/fermentation8050241.
14) Bruce IJ, Sen T. Surface Modification of Magnetic Nanoparticles with Alkoxysilanes and Their Application in Magnetic Bioseparations. *Langmuir*. 2005;21(15):7029–7035. Available from: https://doi.org/10.1021/la050553t.
15) Liu Y, Zhu ZY, Meng XG, Yin HX, Meng MJ, Han J, et al. The Preparation of Aniline Formaldehyde Condensate-Mesoporous Materials Compound and the Application in Adsorption of Zn(II) and Pb(II) in Aqueous Solution. *Advanced Materials Research*. 2013;781-784:2229–2232. Available from: https://doi.org/10.4028/www.scientific.net/AMR.781-784.2229.
16) Deng J, He C, Peng Y, Wang J, Long X, Li P, et al. Magnetic and conductive Fe3O4-polyaniline nanoparticles with core-shell structure. *Synth Met*. 2003;139:166–174. Available from: https://dx.doi.org/10.1016/S0379-6779(03)00166-8.
17) Lowry OH, Rosebrough NJ, Farr AL, Randall RJ. Protein measurement with the Folin phenol reagent. *J Biol Chem*. 1951;193:52451–52457. Available from: https://dx.doi.org/10.1016/s0021-9258(19)52451-6.
18) Fuwa H, , , , and. A New Method For Microdetermination Of Amylase Activity By The Use Of Amylose As The Substrate. *The Journal of Biochemistry*. 1954;41(5):583–603. Available from: https://doi.org/10.1093/oxfordjournals.jbchem.a126476.
19) Augustine M, Madhusudhanan DT, Velayudhan MP. Thermal deactivation studies of alpha-amylase immobilized onto core-shell structured aniline formaldehyde crosslinked polyaniline magnetic nanocomposite. *Biotechnology & Biotechnological Equipment*. 2023;37(1):273–285. Available from: https://doi.org/10.1080/13102818.2023.2182150.
20) Sun X, Zheng C, Zhang F, Yang Y, Wu G, Yu A, et al. Size-Controlled Synthesis of Magnetite (Fe₃O₄) Nanoparticles Coated with Glucose and Gluconic Acid from a Single Fe(III) Precursor by a Sucrose Bifunctional Hydrothermal Method. *The Journal of Physical Chemistry C*. 2009;113(36):16002–16008. Available from: https://doi.org/10.1021/jp9038682.
21) Zhang D, Chen H, Hong R. Preparation and Conductive and Electromagnetic Properties of Fe₃O₄/PANI Nanocomposite via Reverse In Situ Polymerization. *Journal of Nanomaterials*. 2019;2019:1–9. Available from: https://dx.doi.org/10.1155/2019/7962754.
22) Muhammad A, Shah AUHA, Bilal S. Effective Adsorption of Hexavalent Chromium and Divalent Nickel Ions from Water through Polyaniline, Iron Oxide, and Their Composites. *Applied Sciences*. 2020;10(8):2882. Available from: https://doi.org/10.3390/app10082882.
23) Terangpi P, Chakraborty S. Adsorption kinetics and equilibrium studies for removal of acid azo dyes by aniline formaldehyde condensate. *Applied Water Science*. 2017;7(7):3661–3671. Available from: https://doi.org/10.1007/s13201-016-0510-4.
24) Bindu VU, Mohanan PV. Thermal deactivation of α-amylase immobilized magnetic chitosan and its modified forms: A kinetic and thermodynamic study. *Carbohydrate Research*. 2020;498:108185. Available from: https://doi.org/10.1016/j.carres.2020.108185.
25) Silva FS, Pio FS, Ribeiro EJ, De Resende MM. Immobilization of alpha-amylase (Termamyl® 2X) in Duolite® A-568 resin. *Biocatalysis and Agricultural Biotechnology*. 2023;49:102661. Available from: https://proceedings.science/sinaferm/sinaferm-sheb-2019/papers/immobilization-of-termamyl-r-on-duolite-r-a-568-resin?lang=en.
26) Yandri Y, Ropingi H, Suhartati T, Irawan B, Hadi S. Immobilization of α-amylase from Aspergillus fumigatus using adsorption method onto zeolite. *Physical Sciences Reviews*. 2023;0(0). Available from: https://www.degruyter.com/document/doi/10.1515/psr-2022-0258/html?lang=de.
27) Salem K, Jabalera Y, Puentes-Pardo JD, Vilchez-Garcia J, Sayari A, Hmida-Sayari A, et al. Enzyme Storage and Recycling: Nanoassemblies of α-Amylase and Xylanase Immobilized on Biomimetic Magnetic Nanoparticles. *ACS Sustainable Chemistry & Engineering*. 2021;9(11):4054–4063. Available from: https://doi.org/10.1021/acssuschemeng.0c08300.